

# Spectral Properties of Thick Split Ring Resonators in the THz regime

Sher-Yi Chiam<sup>a</sup>, Jiaguang Han<sup>a</sup>, Ranjan Singh<sup>b</sup>, Weili Zhang<sup>b</sup>, Thomas Osipowicz<sup>a</sup>  
and Andrew A. Bettiol<sup>a</sup>

<sup>a</sup>Center for Ion Beam Applications, Department of Physics,  
National University of Singapore, Singapore 117542

<sup>b</sup>School of Electrical and Computer Engineering, Oklahoma State University,  
Stillwater, Oklahoma 74078

## ABSTRACT

We fabricated and studied a planar composite material consisting of sub-wavelength double split ring resonator structures made of Gold on a Silicon substrate. Our measurements reveal a strong transmission dip at 0.6 THz. Experimental and numerical results indicate that there is an Inductor-Capacitor resonance at 0.6 THz, characterized by enhanced electric field strength across the ring gap. Our results also indicate a shift in the resonance to higher frequencies as thickness is increased. Spectral properties of the composite material were measured using THz Time Domain Spectroscopy in the range from 0.1 THz to 3.5 THz. Simulations were carried out using the commercially available electromagnetic solver, Microwave Studio<sup>TM</sup>. Fabrication of the structures was done with Proton Beam Writing, a nanolithography technique based on focused MeV protons. The direct-write technique allowed us to fabricate structures much thicker than otherwise possible. For this work, the ring resonator structures had overall dimensions of 38  $\mu\text{m}$  and a thickness of 8  $\mu\text{m}$  with highly vertical and smooth sidewalls with minimum critical dimensions of 2  $\mu\text{m}$ .

**Keywords:** Metamaterials, Split Ring Resonators, THz TDS, Proton Beam Writing

## 1. INTRODUCTION

### 1.1. Metamaterials

Metamaterials are artificial materials which owe their electromagnetic properties to their physical structure rather than their chemical composition. The field has attracted tremendous research attention in recent years, with the number of publications increasing steadily.<sup>1</sup>

Metamaterials are usually composed of arrays of intricate subwavelength metallic structures possessing considerable capacitance and inductance. These subwavelength structures can result in metamaterials having electromagnetic properties not found in nature, such as negative indexes of refraction. Negative refraction using a metamaterial wedge was first demonstrated using 10 GHz microwaves in the year 2001.<sup>2</sup> The metamaterial used in this landmark experiment consisted of intersecting planar arrays of wires and double Split Ring Resonator (SRR) structures made of copper. Double SRRs were first proposed by Pendry *et al.*<sup>3</sup> They consist of two concentric conducting rings, each split by a gap situated oppositely (See Figure 1). Although the SRRs are themselves made of a non-magnetic material, they can demonstrate a band of negative magnetic permeability ( $\mu$ ) values. This is due to their unique physical structure, which gives rise to considerable inductance and capacitance, leading to Inductor-Capacitor(LC) resonances at specific frequencies. Circulating currents at, or close to, these resonant frequencies result in an effective magnetic response.

Since 2001, much effort was put into fabricating metamaterials at ever higher frequencies. Micro and nanofabrication techniques have been used to scale down the double SRR design, and thus increase the resonant frequencies. There are a number of reports of SRRs being fabricated which have resonant frequencies in the THz regime

---

Further author information: (Send correspondence to Sher-Yi Chiam)

Sher-Yi Chiam: E-mail: phycsy@nus.edu.sg, Telephone: +(65)65167954, Fax : +(65)67776126

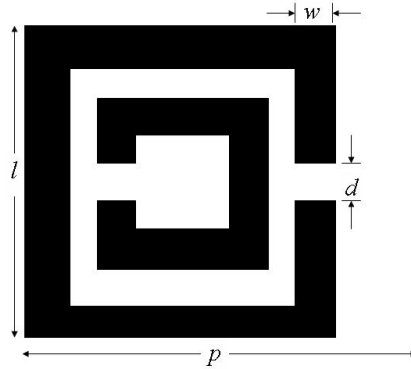


**Figure 1.** Schematic image of a square double SRR which comprises 2 concentric rings, each with a split located oppositely. The dimensions of the SRR reported in this work are as follows:  $l = 38\mu\text{m}$ ,  $t = 6\mu\text{m}$ ,  $g = 3\mu\text{m}$  and  $d = 2\mu\text{m}$ . The thickness of our structures is  $8\mu\text{m}$ . The periodicity of the unit cells in this work,  $p$  is  $50\mu\text{m}$

from 0.1 THz to 10 THz.<sup>4-7</sup> This THz range was quickly surpassed as researchers pursued the goal of achieving negative refraction at optical frequencies. Metamaterial unit cells were simplified to aid nanofabrication. A number of authors used single SRR designs to achieve resonance in the mid-infrared regime.<sup>8,9</sup> Metamaterial designs were then further simplified, and negative refraction at 780nm has been achieved using a “double fishnet” design.<sup>10</sup>

The race towards negative refraction at visible frequencies has perhaps lead researchers to overlook the possible applications of metamaterials at low THz frequencies. Metamaterials often demonstrate prominent pass or reflection bands and thus can be useful for the control and modulation of radiation. For example, Chen *et al* reported the use of a modified SRR array on semiconductor substrate to modulate radiation around 1 THz using an applied bias voltage.<sup>11</sup>

## 1.2. Proton Beam Writing

Proton Beam Writing(PBW) is a direct write lithographic technique for fabricating three-dimensional structures down to and below the 100nm level.<sup>12-14</sup> The technique was developed at the Center for Ion Beam Applications(CIBA) at the Physics Department of the National University of Singapore. PBW utilizes a highly focused beam of megaelectronvolt(MeV) protons to directly write a latent image in a resist. The resist is then chemically developed. PBW works well with the positive resist PolyMethylMethAcrylate(PMMA), as well as the negative resists SU8 (from Microchem) and Hydrogen SilsesQuioxane(HSQ) from Dow Corning. PBW has also been successfully used to fabricate buried channel waveguides on Foturan<sup>TM</sup> photostructurable glass.<sup>15</sup> We are also able to fabricate metallic (Nickel or Gold) nanostructures via an electroforming step where the nano-patterned resist is used as an electroplating mould. The minimum feature size that can be achieved is determined largely by the smallest beam spot size which is well below 100 nm. The smallest feature size achieved using PBW is 22 nm using HSQ resist.<sup>16</sup>

PBW has the ability to fabricate high aspect ratio microstructures in metal or resist. This is because MeV protons will not significantly deviate from a straight line as they travel through the resist. We also have the ability to pattern thick layers of resist, as a 2 MeV proton will penetrate over  $50\mu\text{m}$  of PMMA resist. Although the proton beam generates secondary electrons, these remain very close to the incident beam axis and therefore proximity effects very limited. For these reasons, high aspect ratio structures with vertical and smooth sidewalls can be fabricated using PBW.

## 2. EXPERIMENTAL

### 2.1. Fabrication

For this work we fabricated an array of Au SRRs on silicon substrate. The overall dimension of the array was just over 4 mm by 4 mm. The periodicity of each square unit cell containing one SRR was  $50\mu\text{m}$ . Thus, our array

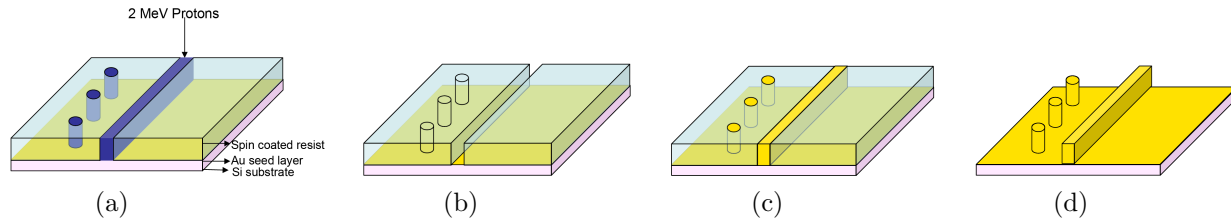


**Figure 2.** Schematic diagram of the fabrication process showing the major steps involved in fabrication. (a) Proton beam writing to define latent images in resist (b) resist development to remove expose(unexposed) resist in the case of a positive(negative) resist (c)electroplating using the patterned resist as a mould and (d) resist removal

consist of over 8000 individual SRRs. All fabrication work was carried out at CIBA at the Physics Department of the National University of Singapore. A schematic diagram of the fabrication process is shown in Figure 2.

The fabrication process began with metallization of 500  $\mu\text{m}$  thick undoped Si substrates. Magnetron sputtering was used to deposit a thin (several nm) layer of Cr as an adhesion layer on a 2-inch Si wafer, followed by an Au layer (about 10 nm thick) which acted as an electroplating seed layer. These wafers were then spin coated with approximately 10  $\mu\text{m}$  of PMMA resist (NANO<sup>TM</sup> PMMA from MicroChem, A11, 950k molecular weight).

Proton Beam Writing was carried out using 2 MeV protons from Singletron 3.5 MeV accelerator. The protons were focused to a spot size of approximately 500 nm. Scanning of the proton beam is achieved using magnetic scan coils (OM 25) which are a part of the Oxford Microbeams scanning system. The scanning is controlled using the Ionscan software, developed in house at CIBA.<sup>17</sup> Beam current was about 10 picoAmperes and was determined using a calibrated detector for Rutherford backscattered ions. The target irradiation dose was 120 nC/ $\text{mm}^2$ . Our scanning system is capable of covering a 400  $\mu\text{m}$  by 400  $\mu\text{m}$  area in a single exposure. Larger areas can be covered using a combination of ion beam scanning and movement provided by an EXFO Burleigh Inchworm Stage.

After exposure, the PMMA resist was developed with a mixture commonly referred to as “GG” developer, which is a mix of several organic compounds (60% diethylene glycol monobutyl ether, 20% morpholine, 5% ethanolamine and 15% water). This is followed by at least 2 rinses with DI water. Gold plating was then carried out using Microfab AU100 gold plating solution (from Enthroner Pte Ltd) at a temperature of 60°C with current density of 2.5 mA/ $\text{cm}^2$ . Under these conditions, plating speed was approximately 1  $\mu\text{m}$  for every 5 minutes.

After plating, the PMMA resist was removed with a Toluene bath at a temperature of 40°C. Finally, the Au seed layer and the Cr adhesion layer were removed to prevent electrical shorting of the structures. This had to be done without damaging the intricate SRR structures. The removal of the Au seed layer was achieved with an Iodine-Potassium Iodide etching solution ( $\text{I}_2$  0.09M, KI 0.6 M). Etch times (usually under 20 seconds) were carefully controlled so as to completely remove the Au seed layer without significant damage to the Au SRR structures. The Cr adhesion layer was then removed using a highly specific Cr etching solution. Again, etch times were carefully controlled to prevent excessive undercutting.

Figure 3 shows optical(a) and scanning electron(b) micrographs of the gold SRRs fabricated for this work. These images were collected after the resist stripping step. From the electron micrographs, the thickness of the SRRs can be clearly seen, as well as the orthogonality and smoothness of the sidewalls.

## 2.2. Characterization and Simulation

Sample characterization was carried out at the School of Computer and Electrical Engineering at Oklahoma State University. Spectra were collected by use of a photoconductive switch-based THz-TDS system, in which four parabolic mirrors arranged in an 8-F confocal geometry.<sup>18,19</sup> A Kerr-lens mode-locked Ti:Sapphire laser capable of generating 26-fs, 86-MHz femtosecond pulses is used as the excitation source of THz-TDS. While this confocal configuration enables an excellent beam coupling between the transmitter and the receiver, a frequency-independent 3.5-mm-diameter terahertz beam waist is achieved which favors the characterization of samples of small dimensions. In this case, the beam covers an area containing several thousand SRRs. The THz-TDS system

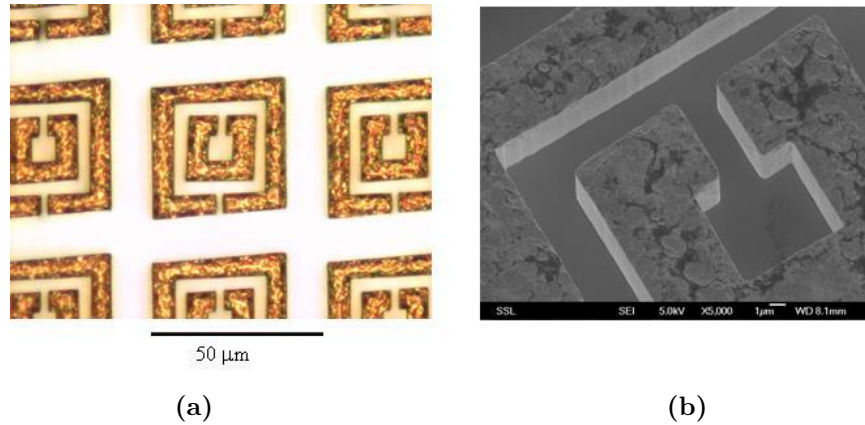


**Figure 3.** Optical (a) and scanning electron (b) micrographs of the gold SRRs fabricated for this work

has a useful bandwidth of 0.1 to 4.5 THz (wavelength from 3 mm - 67  $\mu\text{m}$ ) and a signal to noise ratio (S/N) better than 10000:1. In order to further increase S/N, each curve is an average of six individual measurements. The measurements were carried out with the sample under normal incidence.

Simulations were performed using the commercially available software, Microwave Studio<sup>TM</sup> from Computer Simulation Technologies. These were carried out for a single unit cell, with open boundary conditions at both ends and perfect electrical conductor and perfect magnetic conductor boundary conditions for the sides. From the simulations, we are able to extract a variety of data, the most important of which are the variation of the S21 parameter with frequency, plots of the various components of the electric field, magnetic field and surface current distributions at specific frequencies.

### 3. RESULTS AND DISCUSSION

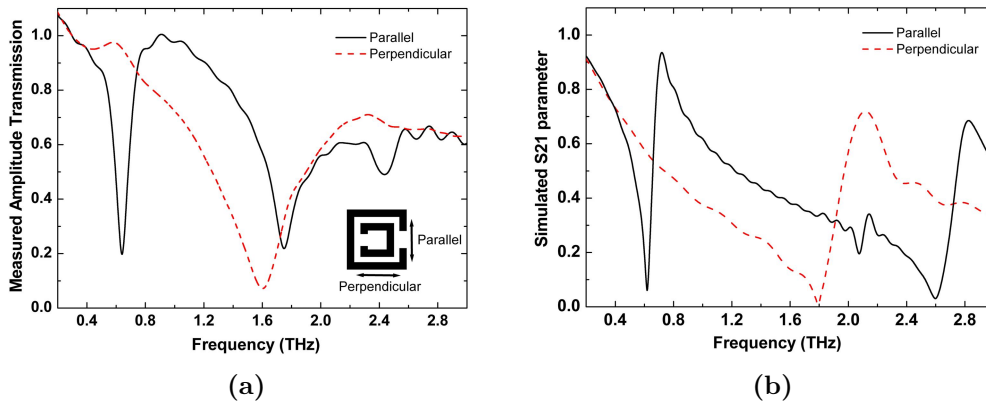


**Figure 4.** Measured transmission amplitude (a) and simulated S21 parameter (b) for our double SRR array. Each graph shows data for 2 orthogonal polarizations. Insert in (a) shows the orientation of the SRR with respect to the electric field for the 2 polarizations. The simulation was able to accurately reproduce the transmission dip at 0.6 THz under the parallel polarization.

Figure 4(a) shows the transmission spectra of our sample, measured with THz TDS. Measurements were made with the sample plane normal to the beam and were carried out for 2 orthogonal polarizations of the electric field. The solid curve in Figure 4(a) shows the measured spectra when the SRRs were orientated with their gap

bearing sides parallel to the electrical field vector of the THz radiation. We define this as the parallel polarization (See insert in Figure 4(a)). For this polarization, there is a prominent dip in the transmission at approximately 0.6 THz. This dip is not present if the sample is rotated 90° such that the electric field is perpendicular to the gap bearing side of the SRR (dashed curve in Figure 4(a)). We were able to reproduce these results with our simulations. In Figure 4(b), a plot of the simulated S21 parameter for both polarizations is shown. Under the parallel polarization, our simulation clearly shows a dip in S21 at 0.6THz (solid curve in Figure 4(b)). The dip is also not present under the perpendicular polarization in our simulation (dashed curve in Figure 4(b)).

Under the parallel polarization, it is expected that oscillating resonant currents can be excited in the SRRs. Although there is no component of magnetic field normal to the plane of the SRR, a LC resonance can be excited due to the coupling of the electric field to the SRRs.<sup>20, 21</sup> This is referred to as the electrical excitation of the LC resonance effect. These resonances cannot be excited under perpendicular polarization. In order to better understand the phenomenon at 0.6 THz, an examination of the simulated electromagnetic fields and the surface currents is instructive. Simulations show that 0.6 THz, the electric field strength across the gap of the outer ring of the double SRR is greatly enhanced (See Figure 5(a)), a feature which is absent at non resonant frequencies. At this frequency, there is a strong magnetic field in a direction normal to the plane of the SRR, although the incoming radiation has no such component (See Figure 5(b)). Figure 6 shows a plot of the surface currents at 0.6 THz. Strong circulating currents are evident along the sidewalls of both the inner and outer rings of the double SRR. In the inner ring, the surface current flows in a continuous loop all round the inside and outside of sidewalls. In the outer ring, there are strong currents on the inside wall, in a direction opposite to the current on the outside wall of the inner ring. There is also some current on the top face of both rings. The magnetic field contributions of all the sidewall currents thus reinforce each other, leading to a strong magnetic field within the inner ring and in the gap between the two rings. These features are absent under the perpendicular polarization. These combination of results clearly point towards a LC resonance at 0.6 THz.

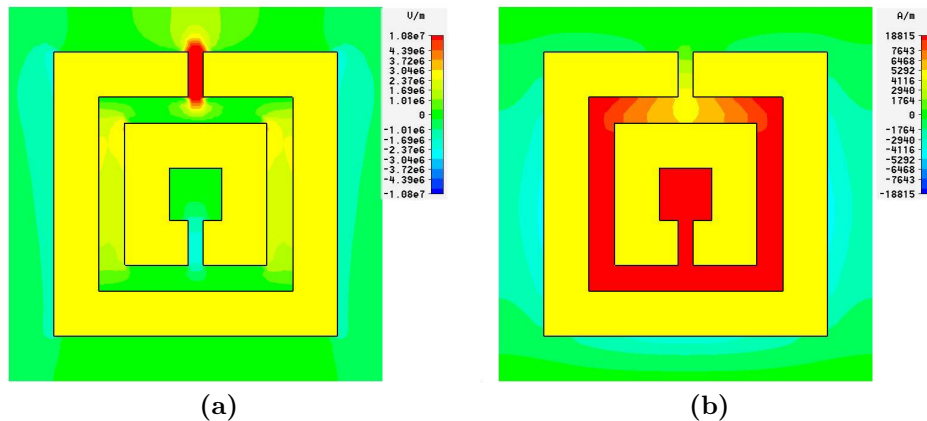


**Figure 5.** Plots of (a) the electric field and (b) the magnetic field across a single SRR at 0.6 THz. The plot of the electric field shows the field component parallel to the gap bearing side of the SRR. The plot of the magnetic field is for the field component normal to the page. The electric field is greatly enhanced across the gap of the outer ring leading to circulating currents that generate significant magnetic field normal to the rings.

It is interesting to note that due to the high aspect ratio capability of PBW, the sidewalls of our structures contribute significant surface area. These sidewalls are also highly vertical and smooth, and thus very close to the model used in our simulations. Current along the sidewalls can thus contribute significantly to the spectral properties of our sample. In almost all studies of SRRs to date, current along the sidewalls is not considered. Rather, it is assumed that the current propagates along the top face of the SRR. Despite the intense interest in metamaterials, relatively few attempts have been made to fabricate high aspect ratio SRRs. Thus, the effects of aspect ratio on the behavior of SRRs should be investigated further. In particular, our simulations indicate that at the inner ring of the double SRR, the current is flowing in a continuous loop around the inside and outside sidewall. Thus, on one ring we have both a clockwise and counter-clockwise current. This is a matter that merits

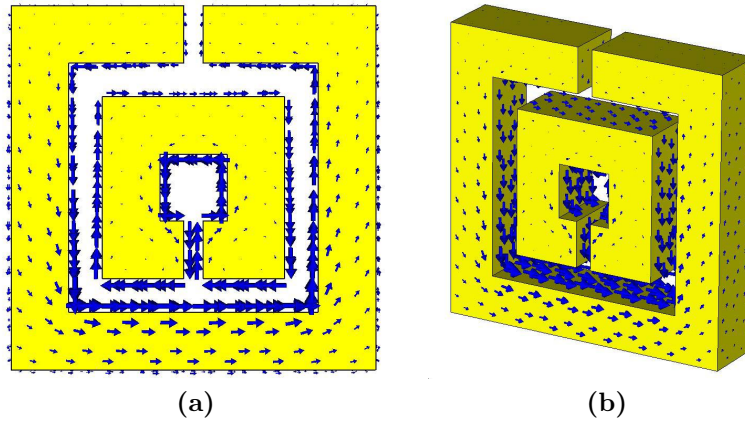


**Figure 6.** Plot and of the surface currents on a single SRR at 0.6. In the top-down view of the surface currents shown in (a), the direction of the currents is clearly seen. In the perspective view shown in (b), it can be seen that there are strong currents on all sidewalls, as well as the top surface of the outer SRR.

further investigation as the typical assumption is one of a unidirectional current along the top surface of an SRR.

Our simulations indicate that as thickness increases, the resonant frequency shift upwards. This trend has been experimentally observed by Guo *et al.*<sup>22</sup> The work of Guo was carried out in frequency range around 100 THz with single SRRs about 500 nm in diameter. The thickness of the SRRs varies from 10 nm to 60 nm. A gradual shift in the frequency of a transmission dip from 90 THz to about 120 THz was noted.

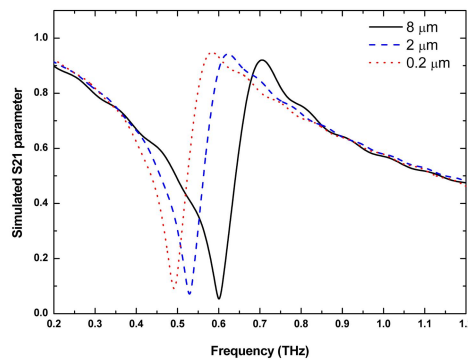


**Figure 7.** Simulated S21 parameter for SRR of varying heights: 8  $\mu\text{m}$  (solid), 2  $\mu\text{m}$  (dotted) and 0.2  $\mu\text{m}$  (dashed).

Figure 7 is a graph showing the frequency dependence of the simulated S21 parameter a double SRR structure of different heights. The lateral dimension are held constant as specified in Figure 1. The height varies from 0.2  $\mu\text{m}$  to 8  $\mu\text{m}$ . The simulated data clearly shows that the dip in the S21 parameter shifts upwards as thickness is increased. At a thickness of 0.2  $\mu\text{m}$ , the simulated data indicates a dip centered at a frequency very close to 0.5 THz, consistent with the experimental data of Azad *et al.*<sup>4</sup> In the work of Azad *et al.*, double SRRs made with very similar lateral dimensions ( $l = 36 \mu\text{m}$  instead of  $38 \mu\text{m}$ ) were fabricated on silicon. The structures had a thickness of about 200 nm. Transmission spectra measured using THz TDS revealed a transmission dip at 0.5 THz. At a thickness of 8  $\mu\text{m}$ , the simulation indicates a dip at 0.6 THz, consistent with the experimental data presented in this work. Additional work to confirm this trend is underway.

## 4. CONCLUSION

We have fabricated and characterized an array of thick double SRRs. Experimental data and simulations clearly indicate the presence of a LC resonance at 0.6 THz. Simulated and experimental data agree well. Our data also indicate that the resonant frequency increases with increasing thickness. The issue of aspect ratio in the spectral properties of SRRs deserves further investigation. Proton Beam Writing offers an attractive fabrication method for this work.

## ACKNOWLEDGMENTS

The work was carried out at the Center for Ion Beam Applications with financial support from the Agency for Science, Technology and Research (A\*STAR) under grant R-144-000-130-112. The Oklahoma State team is supported by the US National Science Foundation. The team from Computer Simulations Technologies (CST) have shared their technical expertise and assisted with our simulations. The authors are especially grateful to Dr Linus Lau, Dr Frank Demming and Mr Chiang Chun Tong from CST.

## REFERENCES

1. V. Vesalago and E. Narimonov, "The left hand of brightness: past, present and future of negative index materials," *Nature Materials* **5**, pp. 759–762, 2006.
2. R. Shelby, D. R. Smith, and S. Schultz, "Experimental verification of a negative index of refraction," *Science* **292**, pp. 77–79, 2001.
3. D. R. J.B Pendry, A.J. Holden and W. Stewart, "Magnetism from conductors and enhanced nonlinear phenomena," *IEEE Transactions on Microwave Theory and Techniques* **47**, pp. 2075–2084, 1999.
4. A. Azad, J. Dai, and W. Zhang, "Transmission properties of terahertz pulses through subwavelength double split ring resonators," *Optics Letters* **31**, pp. 634–636, 2006.
5. T. J. Yen, W. Padilla, N. Fang, D. Vier, D. Smith, J. Pendry, D. Basov, and X. Zhang, "Terahertz magnetic response from artificial materials," *Science* **303**, pp. 1494–1496, 2004.
6. H. Moser, B. Casse, O. Wilhelmi, and B. Saw, "Terahertz response of a microfabricated rod-split-ring-resonator electromagnetic material," *Physical Review Letters* **94**, pp. 063901(1)–063901(4), 2005.
7. N. Katsarakis, G. Konstantinidis, A. Kostopoulos, R. Penciu, T. Gundogdu, M. Kafesaki, E. Economou, T. Koschny, and C. Soukoulis, "Magnetic response of split ring resonators in the far-infrared frequency regime," *Optics Letters* **30**, pp. 1348–1350, 2005.
8. S. Linden, C. Enkrich, M. Wegener, J. Zhou, T. Koschny, and C. Soukoulis, "Magnetic response of metamaterials at 100 thz," *Science* **306**, pp. 1351–1353, 2005.
9. C. Enkrich, D. G. F. Perez-Willard, J. Zhou, T. Koschny, C. Soukoulis, M. Wegener, and S. Linden, "Focused ion beam nanofabrication of near-infrared metamaterials," *Advanced Materials* **17**, pp. 2547–2549, 2005.
10. G. Dolling, M. Wegener, C. Soukoulis, and S. Linden, "Negative-index metamaterial at 780 nm wavelength," *Optics Letters* **32**, pp. 53–55, 2007.
11. H. Chen, W. Padilla, J. Zide, A. T. A.C. Cossard, and R. Averitt, "Active terahertz metamaterial devices," *Nature* **444**, pp. 597–600, 2006.
12. F. Watt, M. B. H. Breese, A. A. Bettiol, and J. A. van Kan, "Proton beam writing," *Materials Today* **30**, pp. 20–29, 2007.
13. J. V. Kan, A. Bettiol, K. Ansari, E. Teo, T. Sum, and F. Watt, "Proton beam writing: a progress review," *International Journal of Nanotechnology* **4**, pp. 464–479, 2004.
14. J. A. van Kan, A. Bettiol, and F. Watt, "Three dimensional nanolithography using proton beam writing," *Applied Physics Letters* **83**, pp. 1629–1631, 2003.
15. A. A. Bettiol, S. V. Rao, E. Teo, J. A. van Kan, and F. Watt, "Fabrication of buried channel waveguides in photosensitive glass using proton beam writing," *Applied Physics Letters* **88**, p. 171106, 2006.
16. J. van Kan, A. Bettiol, and F. Watt, "Hydrogen silsesquioxane a next generation resist for proton beam writing at the 20 nm level," *Nuclear Instruments and Methods in Physics Research B* **260**, pp. 396–399, 2007.

17. A. Bettiol, C. Udalagama, J. van Kan, and F. Watt, "Ionscan: scanning and control software for proton beam writing," *Nuclear Instruments and Methods in Physics Research B* **231**, p. 400406, 2005.
18. W. Zhang, A. Azad, and D. Grischkowsky, "Terahertz studies of carrier dynamics and dielectric response of n-type, freestanding epitaxial gan," *Applied Physics Letters* **82**, pp. 2841–2843, 2007.
19. J. Han, W. Zhang, W. Chen, L. Thamizhmani, A. Azad, and Z. Zhu, "Far-infrared characteristics of zns nanoparticles measured by terahertz time-domain spectroscopy," *Journal of Physical Chemistry B* **110**, pp. 1989–1993, 2006.
20. N. Katsarakis, T. Koschny, M. Kafesaki, E. N. Economou, and C. M. Soukoulis, "Electrical coupling to the magnetic response of split ring resonators," *Applied Physics Letters* **84**, pp. 2943–2945, 2004.
21. M. Kafesaki, T. Koschny, R. S. Penciu, T. F. Gundogdu, E. N. Economou, and C. M. Soukoulis, "Left handed metamaterials: Detailed numerical studies of the transmission properties," *Journal of Optics A: Pure and Applied Optics* **7**, pp. S12–S22, 2005.
22. H. Guo, N. Liu, L. Fu, H. Schweizer, S. Kaiser, and H. Giessen, "Thickness dependence of the optical properties of split ring resonator metamaterials," *Physica Status Solidi* **244**, pp. 1256–1261, 2007.